Published in final edited form as:
J Med Imaging (Bellingham). ; 1(1): 014005–. doi:10.1117/1.JMI.1.1.014005.

Impact of family structure and common environment on heritability estimation for neuroimaging genetics studies using Sequential Oligogenic Linkage Analysis Routines

Mary Ellen Koran[a,b,*], **Tricia A. Thornton-Wells**[a], **Neda Jahanshad**[c], **David C. Glahn**[d], **Paul M. Thompson**[c], **John Blangero**[e], **Thomas E. Nichols**[f], **Peter Kochunov**[g], and **Bennett A. Landman**[h]

[a]Vanderbilt University, Molecular Physiology and Biophysics, Nashville, Tennessee [b]Vanderbilt University, Medical Scientist Training Program, Nashville, Tennessee [c]University of Southern California, Institute of Neuroimaging and Informatics, Imaging Genetics Center, Los Angeles, California [d]Yale University, Psychiatry, New Haven, Connecticut [e]Texas Biomedical Research Institute, Department of Genetics, P.O. Box 760549, San Antonio, Texas [f]University of Warwick, Department of Statistics, Coventry, United Kingdom [g]University of Maryland, Maryland Psychiatric Research Center, Baltimore, Maryland [h]Vanderbilt University, Department of Electrical Engineering, Nashville, Tennessee

Abstract

Imaging genetics is an emerging methodological field that combines genetic information with medical imaging-derived metrics to understand how genetic factors impact observable phenotypes. In order for a trait to be a reasonable phenotype in an imaging genetics study, it must be heritable: at least some proportion of its variance must be due to genetic influences. The Sequential Oligogenic Linkage Analysis Routines (SOLAR) imaging genetics software can estimate the heritability of a trait in complex pedigrees. We investigate the ability of SOLAR to accurately estimate heritability and common environmental effects on simulated imaging phenotypes in various family structures. We found that heritability is reliably estimated with small family-based studies of 40 to 80 individuals, though subtle differences remain between the family structures. In an imaging application analysis, we found that with 80 subjects in any of the family structures, estimated heritability of white matter fractional anisotropy was biased by <10% for every region of interest. Results from these studies can be used when investigators are evaluating power in planning genetic analyzes.

Keywords

heritability; imaging genetics; power calculation; statistical analysis

*Address all correspondence to: Mary Ellen Koran, myemail@university.edu.

1 Introduction

Partitioning and quantification of genetic and environmental factors that influence human development, aging, and pathology are necessary for understanding both normal variability and clarifying biological mechanisms of diseases. For example, genetic factors have been found to affect the formation and operation of brain networks from the micro- to the macroscopic scale[1–4] while common environmental factors influence brain structure volume,[5] liability to schizophrenia,[6] and development of antisocial behavior and conduct disorders.[7] Hence, discovery of neuroanatomical or functional variation that occurs from both common environment and genetic influences is important in studies aimed at teasing apart the etiology of brain development, disease, and disorder.

Sources of individual variability of the cortical landscape are not well understood. Detailed explanation of the causes and consequences of morphological variation in brain structure could have wide significance and numerous implications for neuroscience, psychology, and psychiatry as well as for evolutionary biology. The first step in this direction is to study the proportion of individual variance that can be explained by genetic differences among related individuals. This measurement, called narrow-sense heritability (h^2), is defined as the proportion of total phenotypic variance that is explained by additive genetic factors.

High heritability has already been established for a number of neuroimaging-based phenotypes such as total brain size, gray matter volume, regional gray matter thickness, length of the corpus callosum, and volume of cerebral ventricles.[8] In our recent analyses in one nonhuman primate species (baboons, *Papio hamadryas*), we found high heritability for brain volume ($h^2 = 0.86$; $p < 1e-4$), gray matter volume ($h^2 = 0.67$; $p = 0.01$), and cortical surface area ($h^2 = 0.73$; $p < 1e-3$).[9] The work presented here is an extension of our previous research with the goal of measuring the contribution of intersubject genetic differences to regional variation in the degree of cerebral gyrification.

Genome-Wide Association Studies (GWAS) provide a hypothesis-free framework for discovering genetic polymorphisms associated with a given phenotype, but these studies often necessitate large sample sizes given the generally small effect on trait variance that a single genetic marker may have and the burden of correcting for up to a million tests (or more).[10] In imaging genetics studies, the issue of multiple testing is further magnified by the almost infinite traits that can be analyzed; for example, voxel-wise image analysis can have hundreds of thousands of data points. Heritability analysis permits the prioritization of traits for genetic analysis based on the fraction of unexplained variability in a phenotype due to genetic and common environmental factors. Although it is more feasible to obtain a large sample size for a study of unrelated cases and controls, which can improve the power of GWAS, family studies offer robustness to population substructure issues, and both heritability and common environmental variance can be calculated by examining covariance structures in related individuals. For example, monozygotic (MZ), or identical, twins share 100% of their DNA sequence, while dizygotic (DZ) twins, full siblings, and parent/children pairs all share on average 50%. In contrast, MZ and DZ twins and full siblings who are reared together are expected to share more of a common environment than parent/child pairs, though the amount of sharing is debated and may actually be trait specific.[11] The

expected levels of allele and environment sharing provide an upper bound for comparison with a trait of unknown heritability.

The Sequential Oligogenic Linkage Analysis Routines (SOLAR) software package[12,13] provides extensive capabilities for analyzing heritability and common environment variance of traits within diverse familial structures. Recently, these tools have been extended to improve support and computational efficiency for large-scale neuroimaging data.[14,15] These studies use SOLAR to evaluate the heritability of measures of the brain derived from diffusion tensor imaging which yields quantitative measures sensitive to brain development and degeneration. These heritability estimates can be used in future studies to prioritize which regions of the brain to analyze in genetic studies (i.e., those regions with higher heritiabilities will be prioritized in future studies). The SOLAR package has been theoretically and mathematically validated previously,[16] and herein, we venture to extend this theoretical validation to include validation on modeled datasets (where true heritability is known to us and SOLAR's estimates can be validated against) across different family structures and sizes. We characterize heritability and common environment variance estimates in three commonly collected study designs: MZ and DZ twins, nuclear families, and grandnuclear families. We simulate these family structures and their phenotypes across multiple sample sizes, heritabilities, and common environment variances, and we investigate the bias and the variability of the estimated genetic and common environment variance after analysis of the pedigrees and phenotypes in SOLAR. Results from these studies can be used when investigators are evaluating power in planning genetic analyzes.

2 Theory

Our approach follows the standard practice for empirical characterization of statistical estimators. We first construct a generative model representative of voxel-wise imaging data in the presence of benign confounding effects. Using this model, we simulate known pedigree structures and phenotype (trait) heritability to create finite sample data from known distributions. We iteratively evaluate the estimators and compute the bias (i.e., expected difference between estimated and true heritability values) and variability (i.e., as measured by the standard deviation of the observed heritability values) from 100 iterations.

Analysis of linkage structure with SOLAR is based around the standard additive effects model

$$\mathbf{y}=\mathbf{X}\boldsymbol{\beta}+\boldsymbol{\varepsilon}, \quad (1)$$

where $\boldsymbol{y}$ is the trait vector (1 row per subject), $\mathbf{X}$ is a matrix of observed additive factors (covariates or confounds – 1 row per subject), $\boldsymbol{\beta}$ is a vector (1 row per additive factor) that links additive factors to the trait, and $\boldsymbol{\varepsilon}$ is the unmodeled variance/error term. Importantly,

$$\boldsymbol{\varepsilon}\sim\mathcal{N}(\mathbf{0},\mathbf{2\Phi}\sigma_{\mathrm{a}}^{2}+\boldsymbol{\gamma}\sigma_{\mathrm{c}}^{2}+\mathbf{1}\sigma_{\mathrm{e}}^{2}), \quad (2)$$

where $\mathcal{N}$ is the multivariate Gaussian, **0** is the zero vector (1 row per subject), **Φ** is a matrix of the kinship coefficients between subjects (subjects × subjects), σ_a^2 is the variance attributable to genetics, γ is a matrix of the common environment coefficients between subjects (subjects × subjects), σ_c^2 is the variance attributable to common environment, **1** is the identity matrix (subjects × subjects), and σ_e^2 is the environmental variance (i.e., the remaining unexplained variance). Note that **Φ** codes for the expected fraction of genome shared between subjects (i.e., identical, MZ twins as 0.5, DZ twins and sibling-sibling as 0.25, parent–child as 0.25, grandparent–grandchild as 0.125, etc.). Note that γ codes for an assumed common environment between relationship pairs. For this study, we assumed that children growing up in the same home would be coded as 1, and all other relations would be coded as 0.

The heritability, or relative variance attributable to genetic causes (*A*), is the ratio of σ_a^2 to the residual variance in the traits, which is approximately

$$A \approx \frac{\sigma_a^2}{\sigma_a^2+\sigma_c^2+\sigma_e^2} \quad (3)$$

under the assumption that total phenotypic variance σ_p^2, is the sum of the genetic and environmental variances such that

$$\sigma_p^2 \approx \sigma_a^2+\sigma_c^2+\sigma_e^2. \quad (4)$$

Under these assumptions, *C* is the ratio of the variance contributed by common environmental variance to total variance and *E* is the ratio of the variance due to unique environmental effects and measurement error to total variance, following the ACE model of heritability.[17] The actual computed linear variance may be different from these estimates due to the non-independence of related individuals and reduced degrees of freedom. The SOLAR model is given **X**, β, γ, and **Φ**, and calculates estimates of β, *A*, and *C*.

3 Methods

We evaluated SOLAR's ability to accurately estimate the heritability of a trait in simulated data under one of the three distinct familial structures: (1) twin pairs consisting of equal numbers of DZ and MZ twin sets, (2) nuclear families consisting of two siblings and their mother and father (quartets), and (3) grandnuclear families consisting of two siblings and their mother, father, maternal grandparents, and paternal grandparents (octets). For each family structure, pedigrees and phenotypes were simulated in *R* (http://www.r-project.org/) following simulation structures previously published.[18]

For the simulated twin pedigrees, 2, 5, and 10 to 150 sets (in increments of 10) of two MZ and two DZ twins were modeled [resulting in 8, 20, and 40 to 600 subjects (in increments of 40) total]. For the simulated nuclear family pedigrees, 2, 5, and 10 to 150 quartets (in increments of 10) were modeled [resulting in 8, 20, and 40 to 600 subjects (in increments of

40) total]. For the grandnuclear family pedigrees, to keep total number of subjects relatively similar across the family structures, and to avoid testing only one pedigree, 2, 3, and 5 to 75 octets (in increments of 5) were simulated [resulting in 16, 24, and 40 to 600 subjects (in increments of 40) total].

Within each family structure and sample size to simulate quantitative phenotypes, A was swept between 0 and 0.95 in increments of 0.05 (20 levels), and values for C were iterated along 0, 0.3, 0.5, 0.7, only while $1 - C < A$. Phenotypes were simulated at each combination of A and C 100 times (with 100 Monte Carlo iterations). Multivariate Gaussian noise was generated according to the heritability structure [Eq. (2)] solving for $\boldsymbol{\varepsilon}$. A simulated covariate was randomly generated for each individual ($X \sim U[1, 100]$) and used as an additive factor in Eq. (1) with $\beta = 0.005$ to determine the simulated quantitative phenotype ($\boldsymbol{y}$). The simulated data ($\boldsymbol{y}$), the modeled covariate ($\mathbf{X} = [\mathbf{1}:\boldsymbol{x}]$), the familial structure ($\boldsymbol{\Phi}$), and the common environment matrix ($\boldsymbol{\gamma}$) were passed to SOLAR in phenotype and pedigree file formats. SOLAR estimated A and C for each of the Monte Carlo iterations for every family structure, heritability, and sample size combination using the “polygenic” command.

Bias for the estimates of A and C was calculated as the average estimate across the 100 Monte Carlo simulations for a given combination of A and C minus true A and C modeled, respectively. Variance of the 100 estimates of A and C was calculated as well.

As an example of application in a post hoc analysis, we simulated white matter tract imaging phenotypes (average fractional anisotropy derived from diffusion tensor images) using actual heritability estimates from a large, multisite study[14,15] across the three family structures with reasonable sample size (80 subjects) to showcase expected differences between the three family structures heritability estimates in imaging phenotypes. The same methods as described above were utilized, with A simulated across 14 regions of interest (ROI) (see Table 1 for each ROIs respective A simulated). C was simulated as 0 to keep in consistency with the published results.[14,15] As above, 100 Monte Carlo simulations of phenotypes from each ROI were created and heritability was estimated for each simulation. Bias and variance of the estimates were calculated as well. The average ROI heritability estimates from each family structure were overlaid on the ENIGMA-DTI fractional anisotropy (FA) template and skeleton (www.enigma.ini.usc.edu/ongoing/dti-working-group/) and visualized using MATLAB (http://www.mathworks.com/products/matlab/). The color scale reflects the heritability estimate, with warmer colors suggesting greater heritability.

4 Results

Where $C = 0$ (Fig. 1), heritability estimates produced by SOLAR had absolute biases of < ~0.20 where sample size ~40 subjects or more; this bias was smaller for twin pair data. Twin pairs offered the lowest variance of all study designs. Nuclear and grandnuclear family studies showed higher variability, especially at low subject number. Across all three family structures, at heritabilities <20% with sample sizes < ~80 subjects, heritability was positively biased. Above 20%, heritability was negatively biased in all three study structures

with < ~80 subjects. Beyond heritabilities of 20% with sample sizes above 80 subjects, the three family structures' biases were comparable.

For all simulated datasets where $C > 0$ in all three family structures, estimated heritability measures quickly approached those expected from the simulated data. Where $C = 0.30$, all three family structures' estimates were positively biased at simulated heritabilities of <20%, and negatively biased at simulated heritabilities of greater than 20% when the sample size was <80 subjects (Figs. 2–4). Twin family structure estimates had slightly higher variance with <80 subjects (Figs. 2–4). Where $C = 0.50$ or 0.70, when the sample size was <80 subjects, all three family structures' estimates were still positively biased at simulated heritabilities of <20%. At these same sample sizes, the nuclear and grandnuclear structures were negatively biased at simulated heritabilities of greater than 20%, but twin family structures' estimates remained positively, instead of negatively, biased. Estimates of heritability from twin data again had higher variance. Overall the biases were very low for all three family structures, and the variances were slightly higher in the twin structures than in the nuclear and grandnuclear structures.

For the example application simulating white matter imaging phenotypes, average heritability estimates and bias can be seen in Table 2. In general, with 80 subjects in any of the family structures, estimated heritability was biased by <10% for every ROI. For this simulation, nuclear family structures had slightly higher bias than grandnuclear and twin designs, which is expected based on Fig. 1 results at 80 subjects and heritabilities of around 60% (Fig. 5).

5 Discussion

Prior to this study, the mathematical theory behind SOLAR has been derived and proven,[16] and SOLAR has been applied to large-scale neuroimaging data,[14,15] but SOLAR has not been validated on a dataset with known heritability parameters that it could be compared against. We aimed to extend the theoretical validation of SOLAR to modeled data. With modeled data, true (modeled) heritability was known and we were able to compare SOLAR estimates of heritability to this true value, which was not possible in the previous studies using real data and is an advantage of using modeled data. We were also able to go beyond theoretical validation and apply this system to modeled data, which was modeled based on real imaging data results from prior studies. This analysis has bridged the gap between theoretical validation of mathematical equations and the use of these equations on real data by employing modeled data to validate the algorithms and heritability estimates derived from SOLAR. We were able to show that, in general, the estimates of heritability derived from SOLAR quickly approached the true heritability values across the three family structures as sample size increased, even at small heritabilities and across all values of common environmental contribution to variance. Therefore, when planning imaging genetics studies, imaging scientists can use the SOLAR package to estimate heritability of the imaging phenotype they are interested in, or can use SOLAR to prioritize which imaging phenotype to prioritize for future studies based on the size of the heritability estimate generated, and can use the results from this study to determine how accurate this estimate is based on the appropriate sample size and family design. For example, if a researcher had a

sample of 25 nuclear families and used SOLAR to estimate the heritability of the size of the medial temporal lobe to be ~50% with no common environmental contribution to variance ($C = 0$), this researcher could look at the results from this paper (Fig. 1 in this example) and see that the bias of this result from simulations was ~0 and variance was <0.10. From these conclusions, the researcher can be relatively confident in the estimate derived from SOLAR and could pursue an imaging genetics analysis or grant proposal.

Using the SOLAR heritability estimation package, we characterized heritability estimates by simulating imaging phenotypes across twin, nuclear, and grandnuclear family structures. We simulate these phenotypes across multiple sample sizes, heritabilities, and common environment variances in line with the ACE model of heritability. We investigated the bias and the variance of the estimated heritabilities across these family structures. Overall in this simulation, the estimated heritability values quickly approached the true heritability values as the number of subjects increased, even with small simulated heritabilities across all values of simulated common environmental contribution to variance (C), with comparable bias across the family structures and consistently lower variability in nuclear and grandnuclear family structures. We were also able to simulate imaging phenotypes with previously derived heritability values to showcase how different pedigree structures would result in different heritability estimates in an analysis of heritability of imaging phenotypes. In general, the estimates were relatively similar across the three family structures, but we were able to show how the expected differences between the three family structures heritability estimates would manifest themselves in imaging phenotypes.

These simulations provide a baseline for assessing estimator performance and study power. Under reasonable imaging assumptions of genetic variance, additive effects, common environmental effects, and individual variance or error, the presence or absence of genetic and common environment contribution to a given quantitative phenotype can be reasonably detected for small family-based studies of 40 to 80 individuals. Imaging studies of this size are being routinely undertaken. Thus, heritability analysis of imaging data is imminently feasible if familial sampling is performed.

The limitations of this study stem from the necessity to make assumptions when simulating data. We assumed complete pedigrees, which is perhaps not realistic for experimental datasets. We also assumed an additive genetic model and modeled common environmental covariance between only twins and siblings. In continuing work, we are seeking to improve and expand upon the statistical modeling approach utilized in this study so that we can more readily generalize across potential noise structures and incomplete pedigrees. We are interested in encapsulating these tools so that researchers can better model the impact of their sampling strategies and the propagation of these effects into heritability analysis, and ultimately, better answer the fundamental question of which traits are heritable and therefore, which should be prioritized in genetic analyzes. SOLAR provides an easy to use option for determining genetic and common environment effects in large pedigree structure designs.

Acknowledgments

This work was supported by R01EB15611 (P. K.). N. J. and P. T. were supported by R01 HD050735, EB008432, EB008281, and EB007813 (to P. T.). M. E. K. was supported by T32 GM07347. T. E. N. was supported by R01 EB015611-01 and U54MH091657-03. This work was conducted in part using the resources of the Advanced Computing Center for Research and Education at Vanderbilt University, Nashville, Tennessee. The project described was supported by the National Center for Research Resources, Grant UL1 RR024975-01, and is now at the National Center for Advancing Translational Sciences, Grant 2 UL1 TR000445-06.

References

1. Kochunov P, et al. Genetics of microstructure of cerebral white matter using diffusion tensor imaging. NeuroImage. 2010; 53(3):1109–1116. [PubMed: 20117221]
2. Jahanshad N, et al. Genetic influences on brain asymmetry: a DTI study of 374 twins and siblings. NeuroImage. 2010; 52(2):455–469. [PubMed: 20430102]
3. Tost H, Bilek E, Meyer-Lindenberg A. Brain connectivity in psychiatric imaging genetics. NeuroImage. 2012; 62(4):2250–2260. [PubMed: 22100419]
4. Jahanshad N, et al. Genome-wide scan of healthy human connectome discovers SPON1 gene variant influencing dementia severity. Proc Natl Acad Sci U S A. 2013; 110(12):4768–4773. [PubMed: 23471985]
5. Brun CC, et al. Mapping the regional influence of genetics on brain structure variability—a tensor-based morphometry study. NeuroImage. 2009; 48(1):37–49. [PubMed: 19446645]
6. Sullivan PF, Kendler KS, Neale MC. Schizophrenia as a complex trait: evidence from a meta-analysis of twin studies. Arch Gen Psychiatry. 2003; 60(12):1187–1192. [PubMed: 14662550]
7. Trzesniewski KH, et al. Revisiting the association between reading achievement and antisocial behavior: new evidence of an environmental explanation from a twin study. Child Dev. 2006; 77(1): 72–88. [PubMed: 16460526]
8. Thompson PM, et al. Genetic influences on brain structure. Nat Neurosci. 2001; 4(12):1253–1258. [PubMed: 11694885]
9. Rogers J, et al. Heritability of brain volume, surface area and shape: an MRI study in an extended pedigree of baboons. Hum Brain Mapp. 2007; 28(6):576–583. [PubMed: 17437285]
10. Spencer CCA, et al. Designing genome-wide association studies: sample size, power, imputation, and the choice of genotyping chip. PLoS Genet. 2009; 5(5):e1000477. [PubMed: 19492015]
11. Horwitz AV, et al. Rethinking twins and environments: possible social sources for assumed genetic influences in twin research. J Health Soc Behav. 2003; 44(2):111–129. [PubMed: 12866384]
12. Williams JT, et al. Joint multipoint linkage analysis of multivariate qualitative and quantitative traits. I. Likelihood formulation and simulation results. Am J Hum Genet. 1999; 65(4):1134–1147. [PubMed: 10486333]
13. Williams JT, et al. Joint multipoint linkage analysis of multivariate qualitative and quantitative traits. II. Alcoholism and event-related potentials. Am J Hum Genet. 1999; 65(4):1148–1160. [PubMed: 10486334]
14. Jahanshad N, et al. Multi-site genetic analysis of diffusion images and voxelwise heritability analysis: a pilot project of the ENIGMA-DTI working group. NeuroImage. 2013; 81:455–469. [PubMed: 23629049]
15. Kochunov P, et al. Multi-site study of additive genetic effects on fractional anisotropy of cerebral white matter: comparing meta and mega analytical approaches for data pooling. NeuroImage. 2014; 95:136–150. [PubMed: 24657781]
16. Almasy L, Blangero J. Multipoint quantitative-trait linkage analysis in general pedigrees. Am J Hum Genet. 1998; 62(5):1198–1211. [PubMed: 9545414]
17. Van der Schot AC, et al. Influence of genes and environment on brain volumes in twin pairs concordant and discordant for bipolar disorder. Arch Gen Psychiatry. 2009; 66(2):142–151. [PubMed: 19188536]
18. Feng R, et al. Analysis of twin data using SAS. Biometrics. 2009; 65(2):584–589. [PubMed: 18647295]

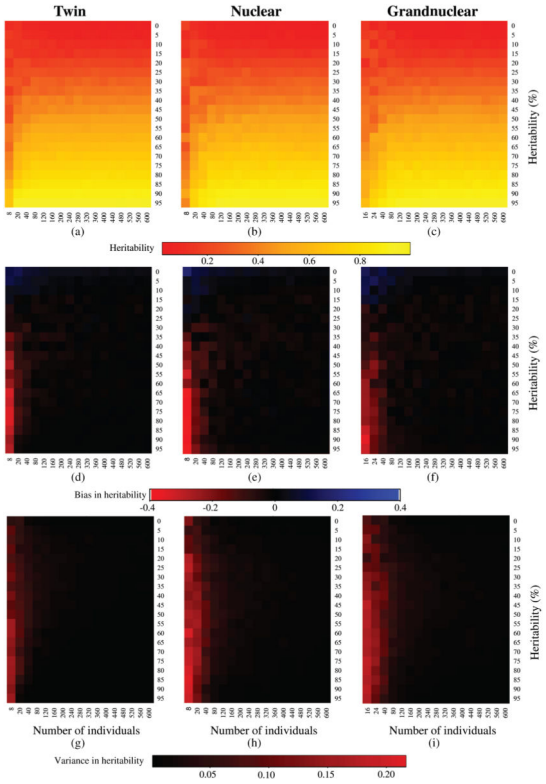

Fig. 1.

Results from the simulation analysis with common environmental contribution to variance (*C*) of 0. The first row plots heritability estimates from the (a) twin, (b) nuclear, and (c) grandnuclear families of varying sample size (*x*-axis, subject number) across the modeled heritabilities (*y*-axis, heritability in percentage modeled). The color scale reflects the heritability estimate, with warmer colors suggesting greater heritability. The middle row plots biasin the heritability estimates from the (d) twin, (e) nuclear, and (f) grandnuclear families of varying sample size (*x*-axis, subject number) across the modeled heritabilities (*y*-axis, heritability in percentage modeled). The color scale reflects the bias of the heritability estimate, with red or blue suggesting greater bias in the negative or positive direction, respectively. The bottom row plots variance in the heritability estimates from the (g) twin, (h) nuclear, and (i) grandnuclear families of varying sample size (*x*-axis, subject number) across the modeled heritabilities (*y*-axis, heritability in percentage modeled). The color scale reflects the bias of the heritability estimate, with red suggesting greater variance in the estimates.

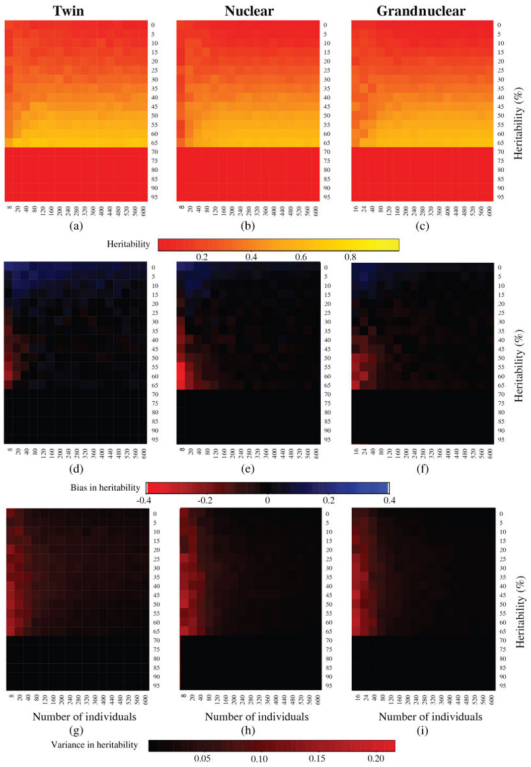

Fig. 2.

Results from the simulation analysis with common environmental contribution to variance (*C*) of 0.30. The first row plots heritability estimates from the (a) twin, (b) nuclear, and (c) grandnuclear families of varying sample size (*x*-axis, subject number) across the modeled heritabilities (*y*-axis, heritability in percentage modeled). The color scale reflects the heritability estimate, with warmer colors suggesting greater heritability. The middle row plots bias in the heritability estimates from the (d) twin, (e) nuclear, and (f) grandnuclear families of varying sample size (*x*-axis, subject number) across the modeled heritabilities (*y*-axis, heritability in percentage modeled). The color scale reflects the bias of the heritability estimate, with red or blue suggesting greater bias in the negative or positive direction, respectively. The bottom row plots variance in the heritability estimates from the (g) twin, (h) nuclear, and (i) grandnuclear families of varying sample size (*x*-axis, subject number) across the modeled heritabilities (*y*-axis, heritability in percentage modeled). The color scale reflects the bias of the heritability estimate, with red suggesting greater variance in the estimates.

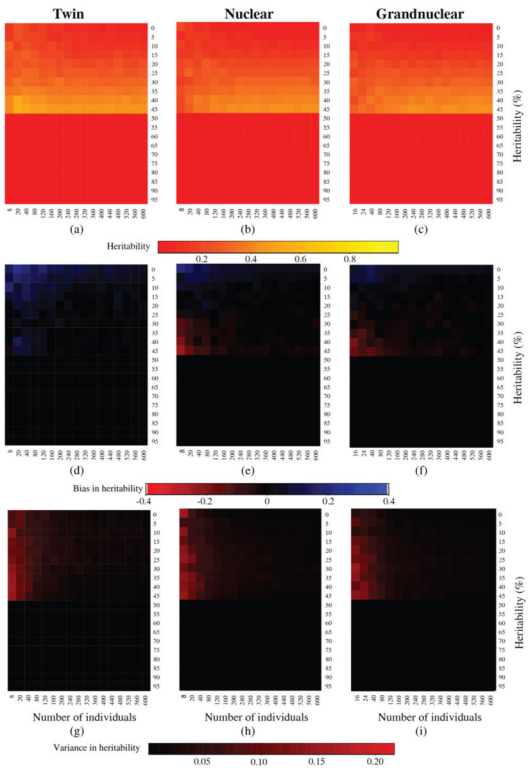

Fig. 3.

Results from the simulation analysis with common environmental contribution to variance (*C*) of 0.50. The first row plots heritability estimates from the (a) twin, (b) nuclear, and (c) grandnuclear families of varying sample size (*x*-axis, subject number) across the modeled heritabilities (*y*-axis, heritability in percentage modeled). The color scale reflects the heritability estimate, with warmer colors suggesting greater heritability. The middle row plots bias in the heritability estimates from the (d) twin, (e) nuclear, and (f) grandnuclear families of varying sample size (*x*-axis, subject number) across the modeled heritabilities (*y*-axis, heritability in percentage modeled). The color scale reflects the bias of the heritability estimate, with red or blue suggesting greater bias in the negative or positive direction, respectively. The bottom row plots variance in the heritability estimates from the (g) twin, (h) nuclear, and (i) grandnuclear families of varying sample size (*x*-axis, subject number) across the modeled heritabilities (*y*-axis, heritability in percentage modeled). The color scale reflects the bias of the heritability estimate, with red suggesting greater variance in the estimates.

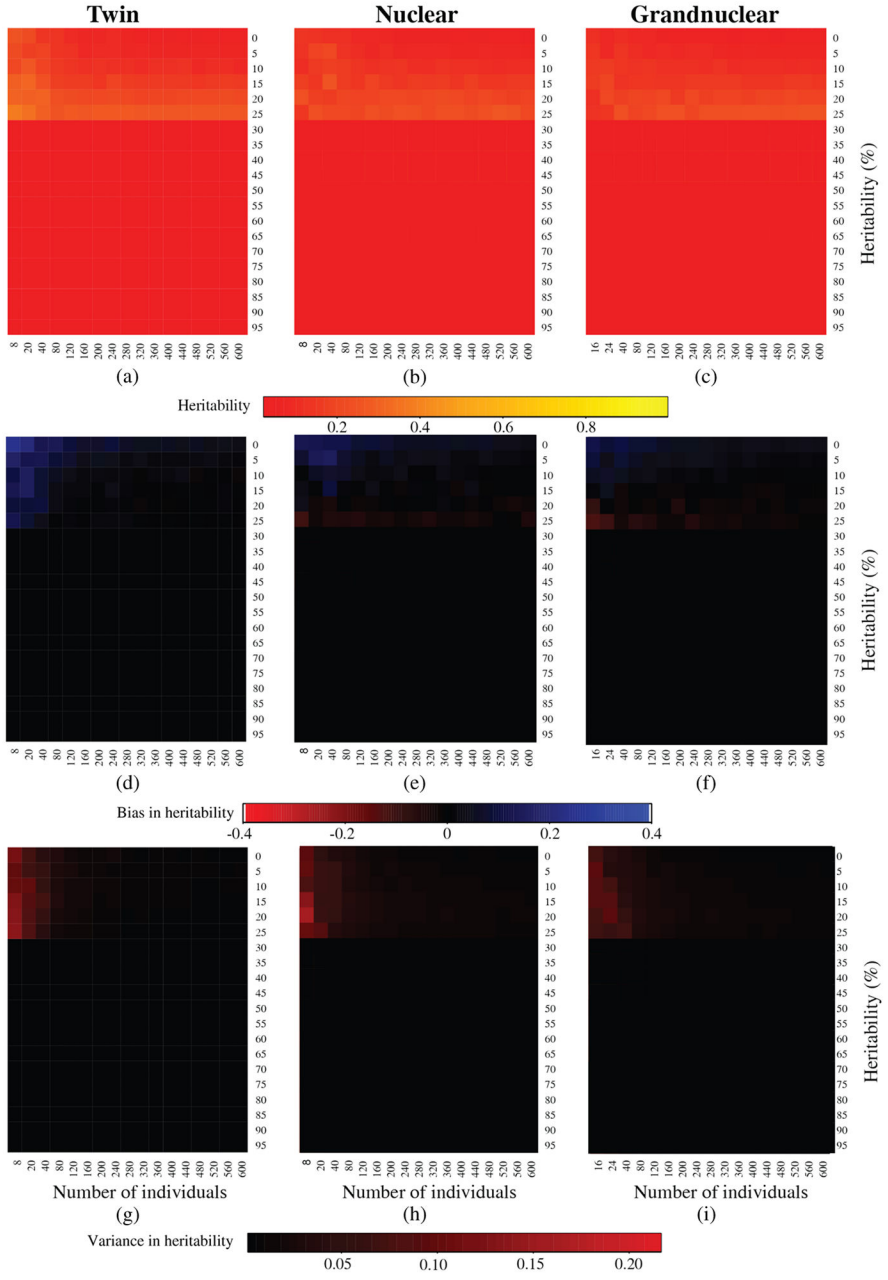

Fig. 4.

Results from the simulation analysis with common environmental contribution to variance (*C*) of 0.70. The first row plots heritability estimates from the twin (a), nuclear (b), and grandnuclear (c) families of varying sample size (*x*-axis, subject number) across the modeled heritabilities (*y*-axis, heritability in percentage modeled). The color scale reflects the heritability estimate, with warmer colors suggesting greater heritability. The middle row plots bias in the heritability estimates from the twin (d), nuclear (e), and grandnuclear (f) families of varying sample size (*x*-axis, subject number) across the modeled heritabilities (*y*-axis, heritability in percentage modeled). The color scale reflects the bias of the heritability

estimate, with red or blue suggesting greater bias in the negative or positive direction, respectively. The bottom row plots variance in the heritability estimates from the twin (g), nuclear (h), and grandnuclear (i) families of varying sample size (*x*-axis, subject number) across the modeled heritabilities (*y*-axis, heritability in percentage modeled). The color scale reflects the bias of the heritability estimate, with red suggesting greater variance in the estimates.

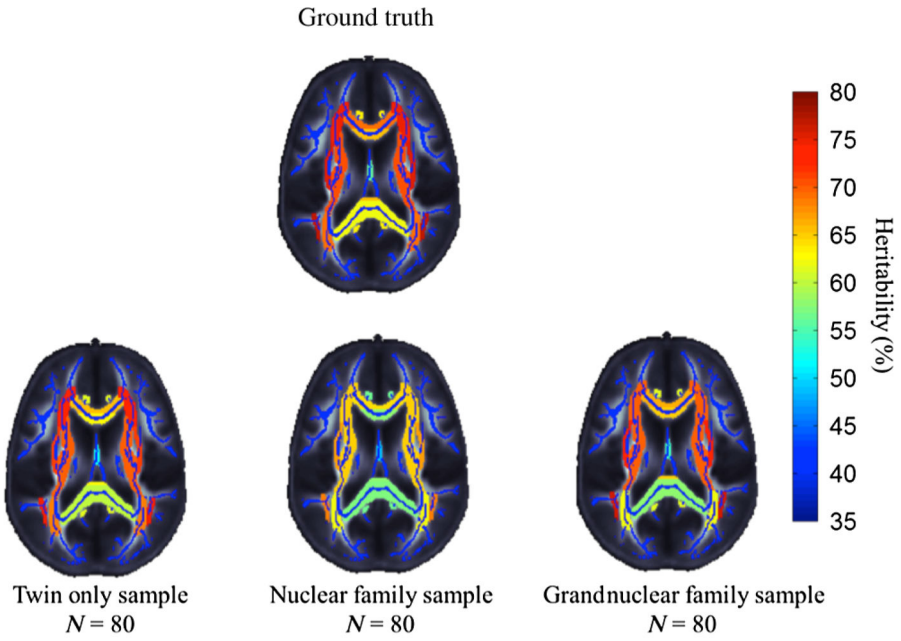

Fig. 5.

Results from the application analysis. Heritability estimates from the twin, nuclear, and grandnuclear families of 80 subjects overlayed on the ENIGMA-DTI fractional anisotropy template and skeleton. The color scale reflects the heritability estimate, with warmer colors suggesting greater heritability. The ground truth heritabilities were derived from the previous literature.[14,15]

Table 1

Regions of interest and the heritability modeled for the application analysis. Heritabilities were derived from the previous literature.[14,15]

Region of interest	Heritability modeled
Body of corpus callosum	0.6935
Cingulum (cingulate gyrus)—L and R combined	0.6344
Corona radiata—L and R anterior and posterior sections combined	0.7475
Corticospinal tract	0.4241
External capsule—L and R combined	0.7539
Fornix	0.5605
Genu of the corpus callosum	0.6575
Internal capsule—L and R anterior limb, posterior limb, and retrolenticular parts combined	0.7092
Inferior fronto-occipital fasciculus—L and R combined	0.7323
Posterior thalamic radiation—L and R combined	0.6944
Splenium of corpus callosum	0.6203
Superior fronto-occipital fasciculus	0.6373
Superior longitudinal fasciculus	0.7685
Sagittal stratum (include inferior longitudinal fasciculus and inferior fronto-occipital fasciculus)—L and R combined	0.6461

Table 2

Results from the application analysis. Regions of interest and the heritability estimates and bias of the estimates from the twin, nuclear, and grandnuclear families of 80 subjects are shown. Heritabilities simulated were derived from the previous literature.[14,15]

Region of interest	Twin A estimate	Twin bias	Nuclear A estimate	Nuclear bias	Grandnuclear A estimate	Grandnuclear bias
Body of corpus callosum	0.660	−0.034	0.643	−0.050	0.667	−0.026
Cingulum (cingulate gyrus)—L and R combined	0.614	−0.021	0.562	−0.072	0.611	−0.023
Corona radiata—L and R anterior and posterior sections combined	0.734	−0.014	0.652	−0.095	0.700	−0.048
Corticospinal tract	0.411	−0.013	0.453	0.029	0.398	−0.026
External capsule—L and R combined	0.717	−0.037	0.673	−0.081	0.730	−0.024
Fornix	0.523	−0.038	0.485	−0.075	0.545	−0.015
Genu of the corpus callosum	0.629	−0.029	0.576	−0.082	0.647	−0.010
Internal capsule—L and R anterior limb, posterior limb, and retrolenticular parts combined	0.697	−0.012	0.650	−0.059	0.700	−0.010
Inferior fronto-occipital fasciculus—L and R combined	0.709	−0.023	0.635	−0.097	0.714	−0.018
Posterior thalamic radiation—L and R combined	0.685	−0.009	0.622	−0.073	0.624	−0.070
Splenium of corpus callosum	0.602	−0.018	0.571	−0.049	0.580	−0.040
Superior fronto-occipital fasciculus	0.606	−0.031	0.536	−0.101	0.621	−0.016
Superior longitudinal fasciculus	0.753	−0.015	0.687	−0.081	0.762	−0.006
Sagittal stratum (include inferior longitudinal fasciculus and inferior fronto-occipital fasciculus)—L and R combined	0.609	−0.037	0.604	−0.042	0.625	−0.021